

Rapid ice discharge from southeast Greenland glaciers

E. Rignot,¹ D. Braaten,² S. P. Gogineni,² W. B. Krabill,³ and J. R. McConnell⁴

Received 12 January 2004; revised 10 March 2004; accepted 14 April 2004; published 25 May 2004.

[1] Interferometric synthetic-aperture radar (InSAR) observations of southeast Greenland glaciers acquired by the Earth Remote Sensing Satellites (ERS-1/2) in 1996 were combined with ice sounding radar data collected in the late 1990s to estimate a total discharge of $46 \pm 3 \text{ km}^3$ ice per year between 62°N and 66°N , which is significantly lower than a mass input of $29 \pm 3 \text{ km}^3$ ice per year calculated from a recent compilation of snow accumulation data. Further north, Helheim Glacier discharges $23 \pm 1 \text{ km}^3/\text{yr}$ vs $30 \pm 3 \text{ km}^3/\text{yr}$ accumulation; Kangerdlugssuaq Glacier discharges $29 \pm 2 \text{ km}^3/\text{yr}$ vs $23 \pm 2 \text{ km}^3/\text{yr}$; and Daugaard-Jensen Glacier discharges $10.5 \pm 0.6 \text{ km}^3/\text{yr}$ vs $10.5 \pm 1 \text{ km}^3/\text{yr}$. The mass balance of east Greenland glaciers is therefore dominated by the negative mass balance of southeast Greenland glaciers ($-17 \pm 4 \text{ km}^3/\text{yr}$), equivalent to a sea level rise of $0.04 \pm 0.01 \text{ mm}/\text{yr}$. Warmer and drier conditions cannot explain the imbalance which we attribute to long-term changes in ice dynamics. **INDEX TERMS:** 0933 Exploration Geophysics: Remote sensing; 1827 Hydrology: Glaciology (1863); 4556 Oceanography: Physical: Sea level variations; 6924 Radio Science: Interferometry; 6969 Radio Science: Remote sensing. **Citation:** Rignot, E., D. Braaten, S. P. Gogineni, W. B. Krabill, and J. R. McConnell (2004), Rapid ice discharge from southeast Greenland glaciers, *Geophys. Res. Lett.*, *31*, L10401, doi:10.1029/2004GL019474.

1. Introduction

[2] Several methods exist to determine the state of mass balance of an ice sheet, and henceforth its present contribution to sea level rise. Here, we address the mass budget method which compares accumulation of snow in the interior with attrition of ice at the ice sheet periphery where it is drained along narrow channels occupied by outlet glaciers [Weidick, 1995]. A large number of glaciers were studied in this manner in the north-west, north, and north-east parts of the Greenland ice sheet using satellite radar interferometry data, ice sounding radar data, laser altimetry data, and a radar altimetry-derived elevation model of the ice sheet [Rignot et al., 2001]. Despite residual uncertainties in snow accumulation, it was concluded that this sector of the ice sheet exhibits a slightly negative mass balance. InSAR observations of a systematic retreat of the glacier grounding lines indicate that ice is thinning along the coast,

while airborne laser altimetry indicates that the interior regions are broadly in balance with accumulation [Krabill et al., 1999].

[3] Here, we apply a similar approach to the glaciers draining the remainder part of the eastern flank of the ice sheet, south of L. Bistrup Bræ, between 62°N and 72°N . Few reliable glaciological data have been collected in this region prior to the 1990s to estimate ice fluxes [Olesen and Reeh, 1969, 1973; Weidick, 1995]. Yet, these glaciers should discharge several times more ice into the ocean than all northern Greenland glaciers combined if they are in a state of mass balance [Reeh, 1985].

[4] Using differential InSAR, we detect no floating glacier sections south of Størstrommen glacier [Rignot et al., 2001], i.e., the glaciers do not develop floating ice shelves and calve at their junction with the ocean. This is a major physical distinction between northern and southern glaciers [Reeh et al., 1999]. In terms of estimating their ice discharge, this means that ice sounding radar data near the glacier fronts are essential to acquire since no ice thickness proxy can be obtained from ice surface elevation in hydrostatic equilibrium.

2. Data and Methodology

[5] The study region spans from 62°N to 72°N , along the east coast of Greenland (Figure 1). Ice discharge is channeled along narrow, fast moving glaciers due to the presence of a high topographic barrier along the coast. The largest glaciers are Daugaard-Jensen, Kangerdlugssuaq, and Helheim glaciers in the northern part. In the south, numerous glaciers (including Heimdal Glacier), flow rapidly through narrow, deep channels. We name this sector south-east Greenland (SEG) herein.

[6] Drainage basins from these 4 sectors are derived from a digital elevation model of the ice sheet [Bamber et al., 2001], starting from the end points of the flux gates. The total area drained by the 3 large glaciers is $147,000 \text{ km}^2$ (Table 1). The southern sector drains an area $38,280 \text{ km}^2$ in size. Ice caps located between Helheim and Kangerdlugssuaq Glaciers and between Kangerdlugssuaq and Vesfjord Glaciers, which do not drain ice from the ice sheet proper, are not included in this study (Figure 1). Similarly, ice discharge from the glaciers between Kangerdlugssuaq and Daugaard-Jensen glaciers (Vesfjord, Rolige Bræ and Harebræ) is not discussed because it should be small (less than $7 \text{ km}^3/\text{yr}$ over an area of $21,000 \text{ km}^2$) and we do not have a good combination of velocity and ice sounding radar data in that area.

[7] Ice velocity is measured using InSAR (Interferometric Synthetic Aperture Radar) from the Earth Remote Sensing Satellites, ERS-1/2, collected in late 1995/early 1996, during the tandem mission (one-day time separation pairs), during the winter season (Table 2). InSAR only measures ice motion in the radar looking direction, i.e., a one-dimensional

¹Jet Propulsion Laboratory, Pasadena, California, USA.

²Radar Systems and Remote Sensing Laboratory, The University of Kansas, Lawrence, Kansas, USA.

³NASA Goddard Space Flight Center, Wallops Flight Facility, Laboratory for Hydrospheric Processes, Wallops Island, Virginia, USA.

⁴Desert Research Institute, Division of Hydrologic Sciences, Reno, Nevada, USA.

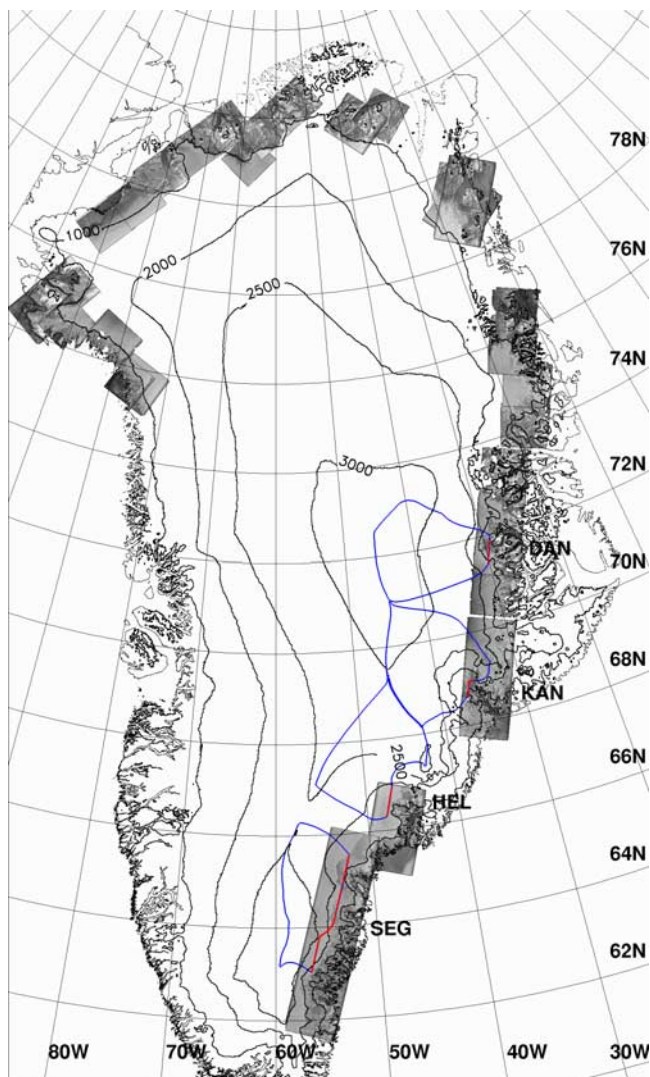


Figure 1. Catchment basin (blue) of 4 glacier areas in east Greenland where glacier discharge was estimated combining InSAR data and ice sounding radar data. The flux gates are shown in red. Elevation contours for 1000, 2000 and 3000 m are shown in black. Radar amplitude images of the ERS-1/2 data used in this study are shown in grey scale (each frame is 120 km × 120 km in size). DAN = Dagaard-Jensen; KAN = Kangerdlugssuaq; HEL = Helheim, and SEG = Southeast Greenland.

component of the velocity vector. No ascending tracks and only descending tracks were available over the study area during that time period. We complemented the InSAR analysis (i.e., phase information in the cross-track

Table 1. Ice Flux (Cubic Kilometer of Ice Per Year) vs Balance Flux (Cubic Kilometer of Ice Per Year) of East Greenland Glaciers

Glacier	Ice flux km ³ /year	Balance flux (area) km ³ /year (km ²)	Mass balance km ³ /year
Dagaard-Jensen	10.5 ± 0.6	10.5 ± 1.0 (48,900)	0 ± 1
Kangerdlugssuaq	29.2 ± 1.7	22.9 ± 2.3 (50,950)	-6 ± 3
Helheim	23.4 ± 1.4	30.0 ± 3.0 (47,150)	+7 ± 3
Southeast Greenland	45.7 ± 2.7	29.1 ± 2.9 (38,300)	-17 ± 4
Total	108.8 ± 3.5	92.5 ± 5 (185,300)	-16 ± 6

Area in column 3 gives the size of each catchment basin. Column 4 shows the mass balance, i.e., column 2 minus column 3.

Table 2. ERS-1/2 Orbit Pairs (Two Pairs Per Glacier) Used in the Study and Corresponding Dates of Acquisition of ERS-1 Data (ERS-2 is One Day Later and its Date is Not Shown)

Glacier	ERS-1/ERS-2 Orbits	Dates
Dagaard-Jensen/ Kangerdlugssuaq	23330/3657, 23831/4158	95/12/31, 96/2/4
Helheim	23960/4287, 23459/3786	96/2/13, 96/1/9
Southeast Greenland	22772/3099, 23273/3600	95/11/22, 95/12/27

direction) of the descending tracks with speckle tracking [Michel and Rignot, 1999] in the along-track direction to form velocity vectors assuming ice flows parallel to the ice sheet surface. The precision of velocity mapping is 5 m/yr in the cross-track direction (InSAR analysis) and 50 m/yr in the along-track direction (speckle tracking). Typical flow velocities are greater than 1 km/yr, so that the error in velocity mapping is less than 5 percent, assuming no temporal variability in ice velocity. Only the component of the velocity normal to the flux gate is used in the calculation of fluxes.

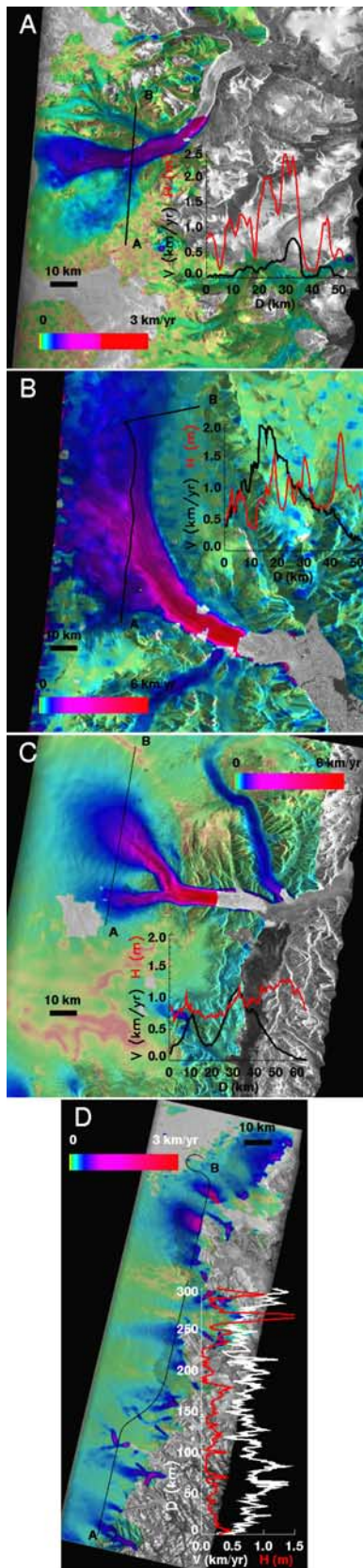
[8] In 1997, ice sounding radar profiles were acquired by the NASA/University of Kansas radar [Gogineni et al., 2001] in east Greenland (Figure 1). In May 2003, new data were acquired across Helheim Glacier, at a higher elevation than in prior attempts which failed to retrieve bottom returns due to the deepness and narrowness of the glacier trough near the coast. Ice thickness is known with a precision of 10 m, or 1 percent of the total thickness. The corresponding uncertainty in ice flux is 6 percent, as listed in Table 1. Ice sounding radar profiles in southeast Greenland and across Helheim glaciers are parallel to the ERS track, so ice fluxes normal to these gates rely on the velocity component which is most accurately known, i.e., parallel to the radar looking direction. The velocity maps and ice thickness profiles of the 4 sectors are shown in Figure 2.

[9] A recent map of snow accumulation [McConnell et al., 2003] is used to calculate mass input to the glaciers over the selected drainage basins. The accumulation data is a hybrid that combines all available ice core and snow pit measurements with the high spatial resolution (0.5°) estimated accumulation from the newly released ERA-40 simulation by the European Centre of Medium-Range Weather Forecasts. Inter-annual variability in net accumulation observed in ice cores and model simulations is significant so the 1990–99 annual average of net accumulation from ERA-40 is used. The direct ice core and snow pit measurements and model simulated net accumulation were objectively combined using co-located co-Kriging on a uniform 20 km grid.

3. Analysis

[10] Snow accumulation over the 4 drainage basins in Table 1 is similar to that derived by Ohmura and Reeh [1991], except in the north where snow accumulation is larger than estimated earlier. This is due to the absence of ice core data in this part of the ice sheet prior to the 1990's.

[11] Ice fluxes in Table 1 reflect an increase in snow accumulation toward the south. Dagaard Jensen Glacier is close to mass balance, Kangerdlugssuaq Glacier exhibits a negative mass budget, and Helheim Glacier, the fastest



moving glacier in east Greenland, exhibits a positive mass budget. Combined together, these glaciers are in balance with snow accumulation.

[12] In contrast, the ice flux from SEG is much larger than snow accumulation, and well above the uncertainty in mass balance. SEG discharges 60 percent more ice than required to maintain the ice sheet in equilibrium, or $17 \text{ km}^3/\text{yr}$. This amount of mass loss is sufficient to raise sea level by $0.04 \text{ mm}/\text{yr}$, using an ice density of 917 kg m^{-3} and a 360 Gt equivalent for each mm of sea level. The negative mass balance of southeast Greenland dominates the mass budget of east Greenland glaciers (Table 1).

[13] During the time period of our observations (November 1995 to February 1996 (Table 2)) we detected no change in ice velocity. Larger velocities could occur in the summer months, in which case the mass balance reported here, based on winter velocities, would be an underestimate.

[14] Our mass balance results are consistent with ice thinning measured with airborne laser altimetry [Krabill *et al.*, 1999; Abdalati *et al.*, 2001] and mass loss estimated from GPS velocity and thickness data at 2000-m elevation [Thomas *et al.*, 2001]. Krabill *et al.* [1999] showed that ice thinning is concentrated at the coast, along the outlet glaciers, is largest nearer to the coast and affects the ice sheet up to the ice divide in southeast Greenland. The mean thinning rate of $285 \text{ mm}/\text{yr}$ estimated by Thomas *et al.* [2001] for a region $34,000 \text{ km}^2$ in size, however, is half the $443\text{-mm}/\text{yr}$ thinning measured here. This suggests that ice thinning is higher at lower elevation, which again is consistent with the airborne laser altimetry surveys.

4. Conclusions

[15] Our mass balance estimates suggest that the glaciers draining southeast Greenland flow faster than required to maintain the ice sheet in a state of mass balance. Surface temperature records of Tasiilq/Ammassalik (at 65.6°N , 37.63°W) near Helheim Glacier show a 1.5°C warming for 1885–1935, followed by 1°C cooling for 1935–1985, a 1°C warming for 1985–2000 [Box, 2002], and sustained warming from 2001 to present. No long-term (century scale) trend in accumulation is found on the ice sheet at ice core locations, although some areas in the south have pronounced 20–40 year cycles. At ice core D1 (64.5°N , 43.5°W), in southeast Greenland, the mean accumulation is $76.2 \pm 17.2 \text{ cm}$ water-equivalent per year over 113 years, with a minimum-maximum of 41.3 and 130. There is a slight increase in accumulation of 0.05 cm water-equivalent per year, however not statistically significant due to a high interannual variability.

[16] This leaves warming and changes in ice dynamics as the potential explanation for the observed imbalance. Drops

Figure 2. Velocity map of (A) Daugaard-Jensen, (B) Kangerdlugssuaq, (C) Helheim, and (D) southeast Greenland glaciers, overlaid on an ERS-1 radar amplitude image. Ice velocity is color coded from brown to yellow, blue and red on a logarithmic scale. Ice sounding radar (ISR) lines used as flux gates are shown in black. The ice velocity and ice thickness along the ISR lines (from A to B) are plotted versus the distance along the line (0 is A) in, respectively, white and brown.

in surface elevation of several meters per year recorded on several east Greenland glaciers cannot be explained by melting alone [Abdalati *et al.*, 2001], and have been attributed to changes in ice dynamics. Such changes may occur as a result of enhanced surface melt water production, which reaches the glacier bed and increases basal lubrication [Zwally *et al.*, 2002]. Enhanced glacier calving may also result from climate warming and accelerate ice flow [Meier and Post, 1987]. Calving glaciers are more sensitive to climate change than glaciers ending on land, and once pushed out of equilibrium by climate may continue their retreat even if climate cools down again. Warmer ocean temperature could also exert an important control on calving [Motyka *et al.*, 2003], which remains to be further explored. Enhanced melt water production and warmer ocean during warmer periods earlier this century or possibly in recent years may have triggered the retreat of calving glaciers along the southeast coast. Weidick [1995] notes little change in the position of the inland ice since the 1930s in that sector. It will be of interest to examine how the calving glaciers of southeast Greenland will react to the sustained warming trend of the 2000's. In the mid 1990s, the glacier changes were pronounced, widespread, and larger than could be explained from the melting of the snow/ice surface in a warmer climate.

[17] **Acknowledgments.** E.R. performed this work at the Jet Propulsion Laboratory, California Institute of Technology, under a contract with the National Aeronautics and Space Administration. Accumulation studies by J.M. were funded by NASA and NSF grants. InSAR data were provided by the European Space Agency over several research contracts.

References

- Abdalati, W., W. Krabill, E. Frederick, S. Manizade, C. Martin, J. Sonntag, R. Swift, R. Thomas, W. Wright, and J. Yungel (2001), Outlet glacier and margin elevation changes: Near-coastal thinning of the Greenland Ice Sheet, *J. Geophys. Res.*, *106*(D24), 33,729–33,742.
- Bamber, J., S. Ekholm, and W. Krabill (2001), A new, high resolution digital elevation model of Greenland fully validated with airborne laser altimeter data, *J. Geophys. Res.*, *106*(B4), 6733–6745.
- Box, J. (2002), Survey of Greenland instrumental temperature records: 1873–2001, *Int. J. Climatology*, *22*, 1829–1847.
- Krabill, W., E. Frederick, S. Manizade, C. Martin, J. Sonntag, R. Swift, R. Thomas, W. Wright, and J. Yungel (1999), Rapid thinning of the southern Greenland Ice Sheet, *Science*, *283*(5407), 1522–1524.
- Gogineni, S., D. Tammana, D. Braaten, C. Leuschen, T. Akins, J. Legardsky, P. Kanagaratnam, J. Stiles, C. Allen, and K. Jezek (2001), Coherent radar ice thickness measurements over the Greenland Ice Sheet, *J. Geophys. Res.*, *106*(D24), 33,761–33,773.
- McConnell, J. R., R. A. Arthern, and S. Das (2003), Accumulation-driven and long-term elevation change on the southern Greenland Ice Sheet, *Eos Trans. AGU*, *84*(6), Fall Meet. Suppl., Abstract C32A-0418.
- Meier, M., and A. Post (1987), Fast tidewater glaciers, *J. Geophys. Res.*, *92*(B9), 9051–9058.
- Michel, R., and E. Rignot (1999), Flow of Moreno Glacier, Argentina, from repeat-pass Shuttle Imaging Radar images: Comparison of the phase correlation method with radar interferometry, *J. Glaciol.*, *45*(149), 93–100.
- Motyka, R., L. Hunter, K. Echelmeyer, and C. Connor (2003), Submarine melting at the terminus of a temperate tidewater glacier, Leconte Glacier, Alaska, USA, *Ann. Glaciol.*, *36*, 57–65.
- Ohmura, A., and N. Reeh (1991), New precipitation and accumulation maps for Greenland, *J. Glaciol.*, *37*(125), 140–148.
- Ohmura, A., P. Calanca, M. Wild, and M. Anklin (1999), Precipitation, accumulation, and mass balance of the Greenland Ice Sheet, *Z. Gletscherkd. Glazialgeol.*, *35*(1), 1–20.
- Olesen, O., and N. Reeh (1969), Preliminary report on glacier observations in Nordvestfjord, East Greenland, *Grønlands Geologiske Undersøgelse*, Report 21, 41–53.
- Olesen, O., and N. Reeh (1973), Glaciological observations in the southwestern Scoresby Sund region, *Grønlands Geologiske Undersøgelse*, Report 58, 49–54.
- Reeh, N. (1985), Greenland Ice Sheet mass balance and sea-level change, in *Glaciers, Ice Sheets, and Sea-Level: Effects of a CO₂-Induced Climatic Change*, pp. 155–171, Nat. Acad., Washington, D. C.
- Reeh, N., C. Mayer, H. Miller, H. Thomsen, and A. Weidick (1999), Present and past climate control on fjord glaciations in Greenland: Implications for IRD-deposition in the sea, *Geophys. Res. Lett.*, *26*(8), 1039–1042.
- Rignot, E., W. Krabill, S. Gogineni, and I. Joughin (2001), Contribution to the glaciology of northern Greenland from satellite radar interferometry, *J. Geophys. Res.*, *106*(D24), 34,007–34,020.
- Thomas, R., B. Csatho, C. Davis, C. Kim, W. Krabill, S. Manizade, J. McConnell, and J. Sonntag (2001), Mass balance of the higher-elevation parts of the Greenland Ice Sheet, *J. Geophys. Res.*, *106*(D24), 33,707–33,716.
- Weidick, A. (1995), Greenland, in *Satellite Image Atlas of Glaciers of the World*, U.S. Geol. Surv. Prof. Pap., *1386C*, C1–C105.
- Zwally, J., W. Abdalati, T. Herring, K. Larson, J. Saba, and K. Steffen (2002), Surface melt-induced acceleration of Greenland ice-sheet flow, *Science*, *297*(5579), 218–222.
- D. Braaten and S. P. Gogineni, Radar Systems and Remote Sensing Laboratory, The University of Kansas, 2291 Irving Hill Road, Lawrence, KS 66045, USA. (gogineni@ittc.ku.edu; pkanagar@ittc.ku.edu)
- W. B. Krabill, NASA Goddard Space Flight Center, Wallops Flight Facility, Laboratory for Hydrospheric Processes, Wallops Island, VA 23337, USA. (krabill@osb1.wff.nasa.gov)
- J. R. McConnell, Desert Research Institute, Division of Hydrologic Sciences, 2215 Raggio Parkway, Reno, NV 89512, USA. (jmconn@dri.edu)
- E. Rignot, Jet Propulsion Laboratory, 4800 Oak Grove Drive, MS 200-227, Pasadena, CA 91109-8099, USA. (eric.rignot@jpl.nasa.gov)